FUNDAMENTAL STUDIES OF NEURAL STIMULATING ELECTRODES

Fifth Quarterly Report
Covering Period August 29, 1995 to November 28, 1995
CONTRACT NO. N01-NS-4-2310

L. S. Robblee
S. F. Cogan
T. L. Rose
U. M. Twardoch
G. S. Jones
R. B. Jones

EIC Laboratories, Inc.
111 Downey Street
Norwood, Massachusetts 02062

Prepared for
National Institutes of Health
National Institute of Neurological
Disorders and Stroke
Bethesda, Maryland 20892

December, 1995

TABLE OF CONTENTS

LIST OF FIGURES

LIST OF TABLES

1.0 INTRODUCTION AND SUMMARY

This report describes the work on NINDS Contract No. N01-NS-4-2310 during the period August 29, 1995 to November 28, 1995. As part of the Neural Prosthesis Program, the broad objectives of the present fundamental studies are: 1) to evaluate the electrochemical processes that occur at the electrode-electrolyte interface during pulsing regiments characteristic of neural prosthetic applications; 2) to establish charge injection limits of stimulation electrode materials which avoid irreversible electrochemical reactions; 3) to develop an *in vitro* method, which can be applied *in vivo*, for determining the electrochemical real area and stability of microelectrodes; 4) to develop new materials which can operate at high stimulation charge densities for microstimulation; and 5) to provide electrochemical and analytical support for other research activities in the Neural Prosthesis Program at NINDS.

Ir microelectrode stability studies were initiated with a U. Michigan probe which has an integrated ribbon cable and Microtek connector rather than the PC board mount of previously tested probes. Cyclic voltammetry studies utilizing mass transport of Ru hexaammine indicate good dimensional stability over 35 days of soaking. However, a 68% increase in electrochemical surface area based on apparent capacitance was observed over the same time frame. Cyclic voltammograms acquired over a wide potential window displayed the symmetrical current peaks representative of activated Ir on 4 of the 6 sites on the probe, even though none of the sites had been intentionally activated. Impedance spectroscopy data were also consistent with the presence of Ir oxide. Future studies of these probes will focus on determining how and when the Ir sites become "activated".

SEM examination of the dual hat-pin Ir microelectrode, which was the subject of the two previous reports, illustrated that one of the electrode tips was severely bent and the Parylene was separated from the Ir surface thereby increasing the length of exposed metal. This observation is consistent with electrochemical data which indicated an increase in electrochemical surface area measured after 130 days of soaking. Possibly the electrode tip was physically damaged by accidental contact with one of the other cell components while preparing the cell for electrochemical measurements, and this contact also produced the damage to the Parylene. The severity of the damage seen by SEM is consistent with this hypothesis. The SEM examination

also revealed the longitudinal groove in the wire which has been reported previously by others as well as by EIC Laboratories. This groove is due to a manufacturing defect in the wire.

Charge injection studies were carried out using video microscopy to supplement observation of potential excursions to determine charge densities for gas bubble formation. Video microscopy also allows the observation of the distribution of gas bubbles on the surface to obtain information about the uniformity of current density distribution. With stimulation of activated Ir sites at a charge density sufficient for bubble formation, bubbles were formed at only a few loci at the edge of the Ir site. Stimulation of unactivated Ir resulted in bubbles completely ringing the edge of the site. The localization of bubbles to the edges of the sites is consistent with a non-uniform current distribution with the edges typically having the highest current density. During these tests, an activated Ir site became slightly darker in color (more activated), and CVs showed an increase in oxide charge capacity supporting the video observation. An unactivated Ir site also became very dark during a period of high charge density stimulation, with post-stimulation CVs showing very large oxide current peaks. The technique not only provides insights about current density distribution, but also identifies changes in Ir activation levels.

2.0 Ir MICROELECTRODE STUDIES

U. Michigan Multi-Site Probe with Ribbon Cable

During this quarter we initiated studies of the stability of Ir sites on probes with integrated ribbon cables received from U. Michigan. The integrated ribbon cables will permit us to carry out long term soaking studies without any structures other than those fabricated on the wafer being exposed to the electrolyte solution and thereby avoid the previous problems with electrolyte penetration beneath the epoxy encapsulant covering the contact pads. Figure 2.1 is a diagrammatic representation of the probe with the sites labeled according to our numbering scheme.

Figure 2.1 Diagrammatic representation of sites and site identification on U. Michigan ribbon cable-probe.

A cell assembly was fabricated which enables a ribbon cable-probe to be held semi-permanently in the cell with a constant level of immersion into the electrolyte and without danger of damage by inserting and removing the reference electrode and gas bubbler. The ribbon cable holder has a capillary tube extending into the cell, and the ribbon cable extends through this tube into the electrolyte. The tube prevents the ribbon from flexing too much in solution and protects it from inadvertent contact with other cell components.

The electrochemical studies completed this quarter included cyclic voltammetric measurements over a range of scan rates with and without Ru hexaammine dissolved in phosphate-buffered saline, pH 7.3 (PBS). Impedance spectroscopy studies were performed in PBS and included frequency dispersion of the impedance magnitude and phase angle with the Ir site potentiostated at a potential equal to its open circuit (equilibrium) potential. Additional impedance measurments were made with the Ir biased at non-equilibrium potentials ranging from

-0.2 V to −0.5 V vs. Ag/AgCl during the impedance measurements. The reason for this was to evaluate whether the impedance of "unactivated" Ir sites is sensitive to impedance. During the periods between electrochemical measurements, the probe remained soaking in PBS solution.

Results

Cyclic Voltammetry Studies

Table 2.1 lists the voltammetric data for the first scan rate study. The background corrected voltammograms obtained at the slowest scan rates of 0.001 and 0.002 V/s did not have a typical sigmoidal shape so that an accurate measure of the reduction current could not be obtained. Voltammograms obtained at 0.005 V/s and 0.01 V/s were sigmoidal with maximum currents independent of scan rate. This steady state behavior is not expected for a site geometry of a rectangle. However, using the steady state current of 4.8 nA observed at 0.005 and 0.01 V/s, an electrochemical radius of 13.5 μm can be calculated using the equation for an ultramicrodisk electrode. At scan rates above 0.02 V/s, currents varied with scan rates as did the current function, $i_p v^{-1/2}$. A limiting value of the current function indicative of linear diffusion was not obtained within the range of scan rates for which background-corrected voltammograms were available. However, the plot of the current function, $i_p v^{1/2}$, vs. $v^{1/2}$ was linear over the range of scan rates 0.005- 0.5 V/s, characteristic of non-linear diffusion, so that the radius and area of the site could be determined from the intercept and slope, respectively, as described previously [1]. This calculation resulted in a value of 4 μm for the radius and 278 μm^2 for the area.

The voltammetric data for the second scan rate study on site 1, carried out after 7 days soaking in PBS, are given in Table 2.2. In this study, voltammograms obtained at scan rates from 0.001 to 0.05 V/s were sigmoidally shaped with maximum currents independent of scan rate. As was observed for the first scan rate study, the observation of steady state currents is not expected for a rectangular geometry. Using the average value of 4.5 nA for the steady state current in the equation for the current at a disk electrode, a value of 13.8 μm is obtained, nearly identical to that obtained in the first scan rate study. The plot of $i_p v^{1/2}$ vs. $v^{1/2}$ was linear over the range of scan rates 0.001 - 1 V/s. From this plot, the radius was calculated to be 5.4 μm, and the calculated area was 365 μm^2. These values are only slightly different from those obtained in the first scan rate study.

Table 2.1 Cyclic voltammetric data for the reduction process in the solution of 1.38 mM $Ru(NH_3)_6Cl_3$ in PBS buffer solution at U. Mich. Ribbon 1, site 1. Study 1

Scan Rate, v (V/s)	Peak Potential ^aE_p (V)	Peak Potential ^aE_p (V)	Half-Wave Potential $^bE_{p/2}$ (V)	i_p (A)	Current Function $i_p v^{-1/2}$ ($AV^{-1/2}s^{1/2}$)
0.001	no peak	no peak			
0.002	"	"			
0.005	"	"	-0.19	4.800E-09	6.789E-08
0.01	"	"	-0.19	4.800E-09	4.80E-08
0.02	"	"	-0.19	5.000E-09	3.536E-08
0.05	"	"	-0.19	5.200E-09	2.328E-08
0.1	"	"	-0.19	5.400E-09	1.708E-08
0.2	"	"	-0.19	5.900-09	1.319E-08
0.5	"	"	-0.19	6.40E-09	9.050E-09

Potential, E vs. Ag/AgCl/3 M NaCl

Table 2.2 Cyclic voltammetric data for the reduction process in the solution of 1.32 mM $Ru(NH_3)_6Cl_3$ in PBS buffer solution at U. Mich. Ribbon 1, site 1. Study No. 2.

Scan Rate, v (V/s)	Peak Potential ^aE_p (V)	Peak Potential ^aE_p (V)	Half-Peak Potential $^bE_{p/2}$ (V)	i_p (A)	Current Function $i_p v^{-1/2}$ ($AV^{-1/2}s^{1/2}$)
0.001	no peak	no peak	-0.19	4.400E-09	1.392E-07
0.002	"	"	-0.19	4.600E-09	1.029E-07
0.005	"	"	-0.19	4.400E-09	6.223E-08
0.01	"	"	-0.19	4.600E-09	4.600E-08
0.02	"	"	-0.19	4.400E-09	3.112E-08
0.05	"	"	-0.19	4.600E-09	2.059E-08
0.1	"	"	-0.19	5.000E-09	1.582E-08
0.2	"	"	-0.19	6.200-09	1.386E-08
0.5	"	"	-0.19	8.75E-09	1.237E-08
1	"	"	-0.19	9.50E-09	9.500E-09

Potential, E vs. Ag/AgCl/3 M NaCl

In both scan rate studies, the voltammograms in PBS generally had larger residual currents at scan rates above 1 V/s than did the voltammograms acquired in Ru hexaammine solution. Because of this disparity the voltammograms for Ru hexaammine reduction could not be corrected for background processes, making it impossible to use the mass transport data at scan rates greater than 1 V/s for calculation of electrochemical dimensions. However, the residual current at 0 V vs. Ag/AgCl in the two scan rate studies provides information regarding the stability of the apparent capacitance and *vida infra*, the electrochemically available surface area. Plots of the residual current at 0 V vs. Ag/AgCl vs. scan rate are shown in Figure 2.2 for the two complete scan rate studies plus an additional study in which voltammograms were acquired only in PBS. Figure 2.3 gives plots of the apparent capacitance calculated from the residual current vs. scan rate. Except for a few anomalous data points in study 2, the data indicate a slight increase in residual current and capacitance between study 1 and 2, but little additional change after study 2.

The electrochemically determined dimensions obtained in the three studies are listed in Table 2.3. The values for electrode radius determined from the transient electrochemical data are much lower than those obtained from the steady state data. The different values may be due to incorrect assumptions about the geometry of the site. For example, the equation used for the steady state current describes diffusion to a disk electrode, not a rectangle. However, even with caveats about electrode geometry, the similarity of the mass transport data in the two studies indicates that there was very little change in the electrode dimensions during the soaking period (Figure 2.4). The ESA, calculated from apparent capacitance at 200 V/s, increased from 1590 μm^2 to 2520 μm^2 in the 8 days between studies 1 and 2. During the next 27 days, the ESA increased only slightly to 2680 μm^2.

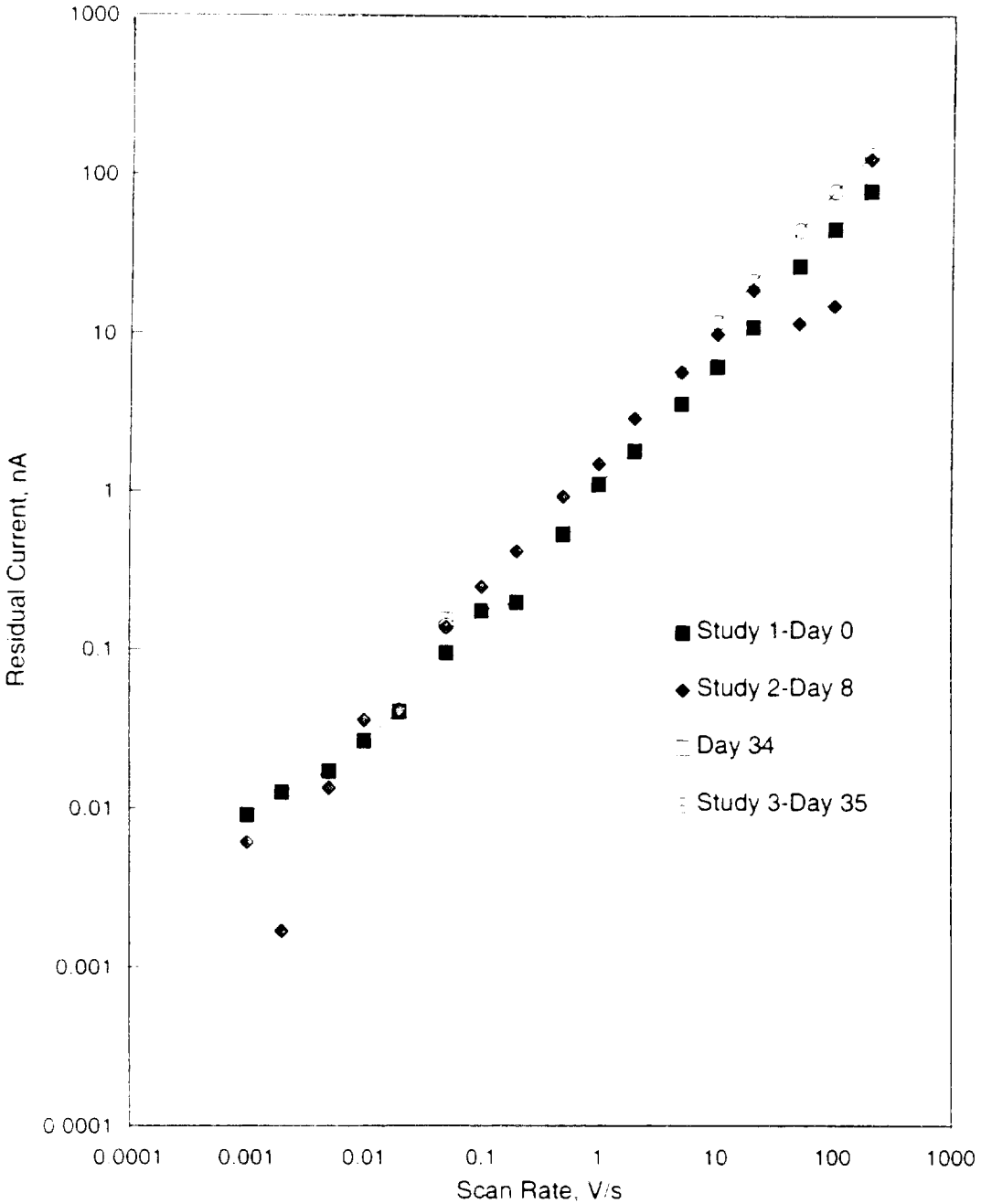

Figure 2 2 Comparison of residual currents at 0 V vs Ag AgCl in two scan rate studies of site 1 on a U Michigan ribbon cable-probe

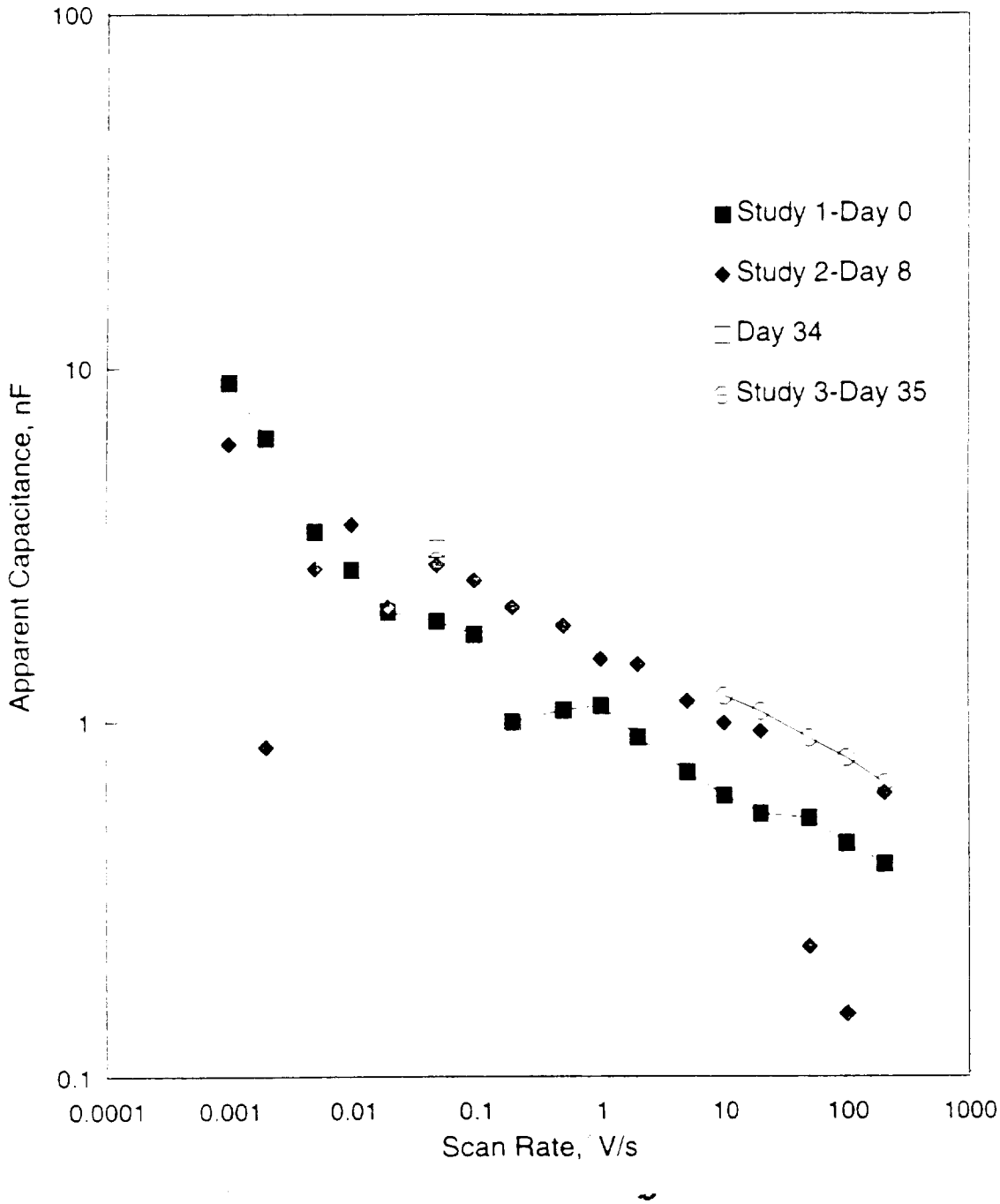

Figure 2.3 Comparison of Capp determined in two scan rate studies of site 1 on a U Michigan ribbon cable-probe

Table 2.3 Dimensions of Ir site No. 1 on U. Michigan Ribbon Cable No. 1

Study No., Soak Time	Dimensions (nominal)			Dimensions from Electrochemical Measurements				
				Steady State[A]		Spherical Diffusion[B]		from C_{app}[C]
	l, µm	w, µm	A - µm²	r, µm (disk)	A - µm² (disk)	r - µm	A - µm²	A - µm²
Study 1, 1-2 days	40	15	600	13.5	572	4.1	278	1590
Study 2, 7-8 days	40	15	600	13.2	547	5.4	365	2520
Study 3,	40	15	600					2680

Footnotes to the table

A Values for r are obtained from the steady state currents obtained at 0.005 and 0.01 V/sec for study 1 and the average of steady state currents obtained at 0.001 to 0.05 V/s for study 2, according to the relationship $r = i_{ss}/4nFCD$. The values for A are calculated using the electrochemically determined value of r in the formula for area of a circle. This value is for comparison only since the electrodes in question are rectangles, not disks.

B A and r are obtained from the slope and intercept of the linear portion of a plot of $iv^{-1/2}$ vs. $v^{-1/2}$ over the range of sweep rates from 0.001 - 0.5 V/s in study 1 and from 0.001 to 1 V/sec in study 2. Data from faster scan rates could not be corrected for background due to inequality of residual currents with and without the depolarizer.

C C_{app} is calculated from the residual current at 0 V (in PBS) at the highest scan rate employed, generally 200 V/sec, using the relationship $C_{app} = i_r/v$. Area is determined from C_{app} assuming a value of 25 µF/cm² for the capacitance of the Ir metal surface.

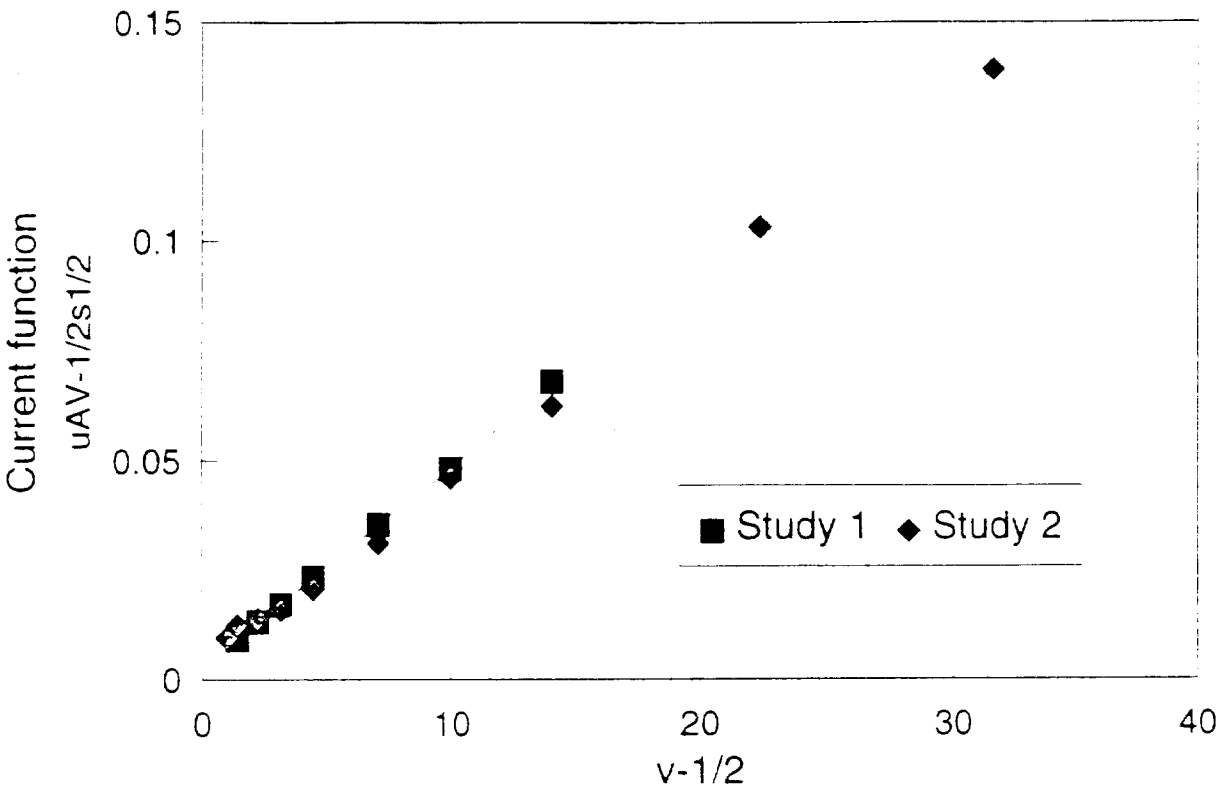

Figure 2.4 Comparison of mass transport data obtained in two scan rate studies of site 1 on a U Michigan ribbon cable-probe

Figure 2.5 illustrates background voltammograms (CVs) acquired in PBS on two different days during two scan rate studies. The scan rate shown, 0.05 V/s, is the only one that is repeated several times during a study. Therefore, it is the only scan rate at which any differences in voltammetric behavior might be discovered. Looking first at the series of CVs on the first day the probe was immersed in PBS, the first CV of the day shows a wave of cathodic current beginning at -0.1 V vs. Ag/AgCl and reaching a plateau at about -0.2 V. This current gradually diminished as successive CVs were acquired until the form identified as CV#7 was observed. This is the more typical shape for a CV in deaerated PBS. The final CV on this day has slightly less current in the potential region between 0.0 V and -0.2 V, but otherwise is very similar to CV#7. Note that the residual current at 0.0 V is nearly the same in the three CVs shown for that day's experiments, in spite of the different currents during the cathodic potential scan.

The CVs acquired on day 8 show greater variation from the first to the last CV. The initial CV shows a broad current peak of cathodic current at -0.2 V. This peak gradually diminished with successive CVs, but was replaced by two small, broad waves of cathodic current as shown in CV#7. At the end of the study when the final CV was acquired, the CV shape was changed again to that shown as the "final CV". The cathodic scan on the final CV had a plateau of cathodic current between 0.1 V and -0.1 V with a large increase in cathodic current as the potential was scanned beyond -0.2 V. The increase in cathodic current might be expected in a CV acquired in oxygen-containing solutions but is usually not seen in CVs taken in a deaerated solution. Possibly there was insufficient deaeration at the time the final CV was acquired. The ribbon cable floats near the top of the solution and the gas space above the solution which may be susceptible to incoming air if the bubbler is turned off for too long a time. Moreover, the Ir site selected for the study is at the upper portion of the probe and therefore just beneath the meniscus.

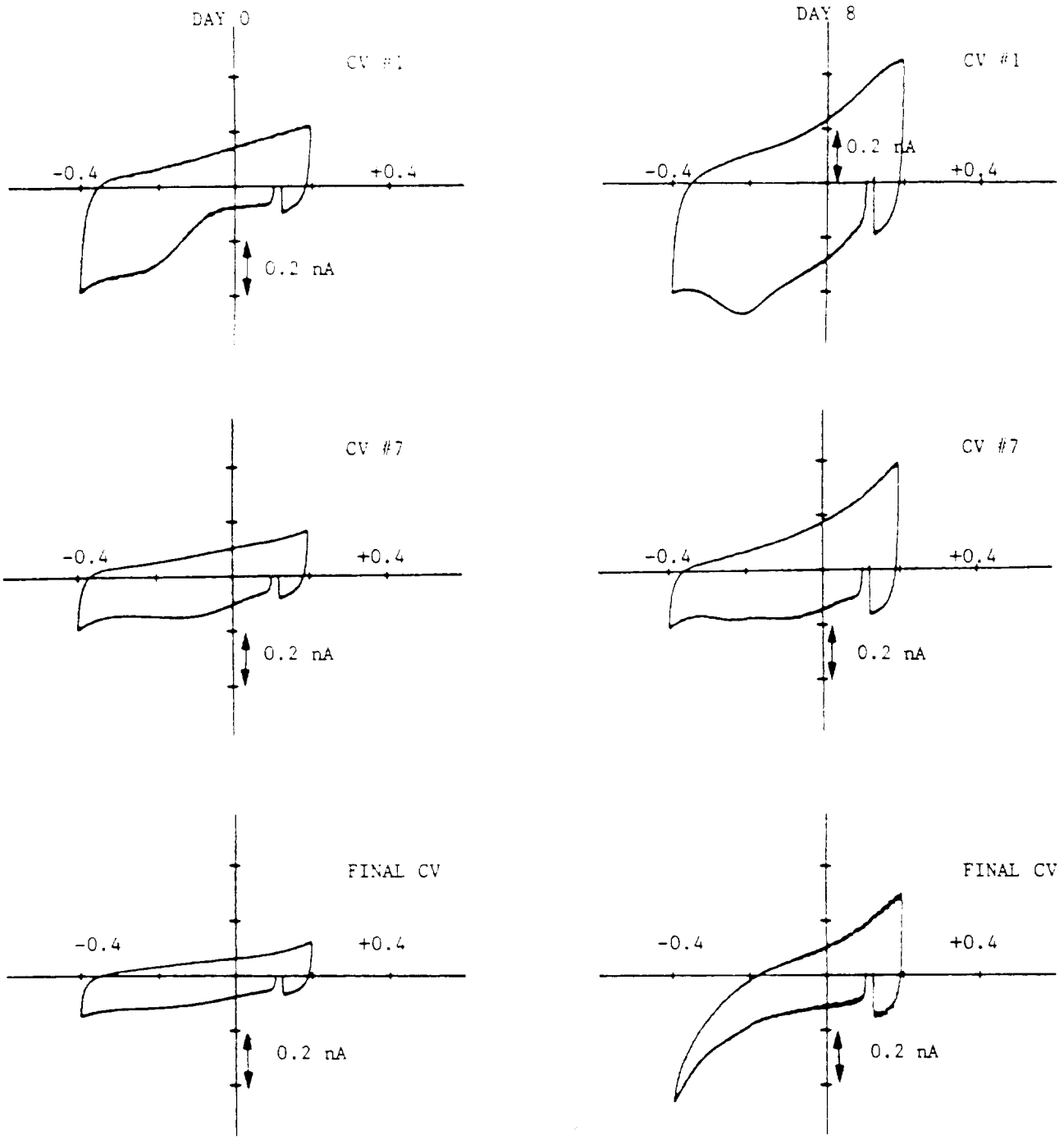

Figure 2.5 Comparison of background voltammograms acquired at site 1 on a U. Michigan ribbon cable-probe during two scan rate studies. Electrolyte: deaerated PBS. Scan rate: 0.05 V/s. Potential scale vs. Ag/AgCl.

The apparent sensitivity of the site to oxygen led us to acquire a series of CVs under different conditions of electrolyte deaeration. In this investigation we focussed on the residual current at 0 V vs. Ag|AgCl because that is the parameter that is assumed to represent capacitive processes only, without contribution from faradaic processes. In work with previous Ir microelectrodes, both wires and sputtered sites on silicon probes, there was no observed effect of oxygen on residual current at 0 V. Figure 2.6 is a plot of residual current vs time of deaeration of electrolyte with Ar, and demonstrates a significant change in current depending upon duration of deaeration. It is not clear at this time why this site has this sensitivity, but the result is consistent with previous, but unreported, experimental observations that a much longer period of deaeration than usual was required to obtain a stable CV at this site in the Ru hexaammine solution. It now seems possible that the problem was related to residual oxygen contributing to the faradaic current.

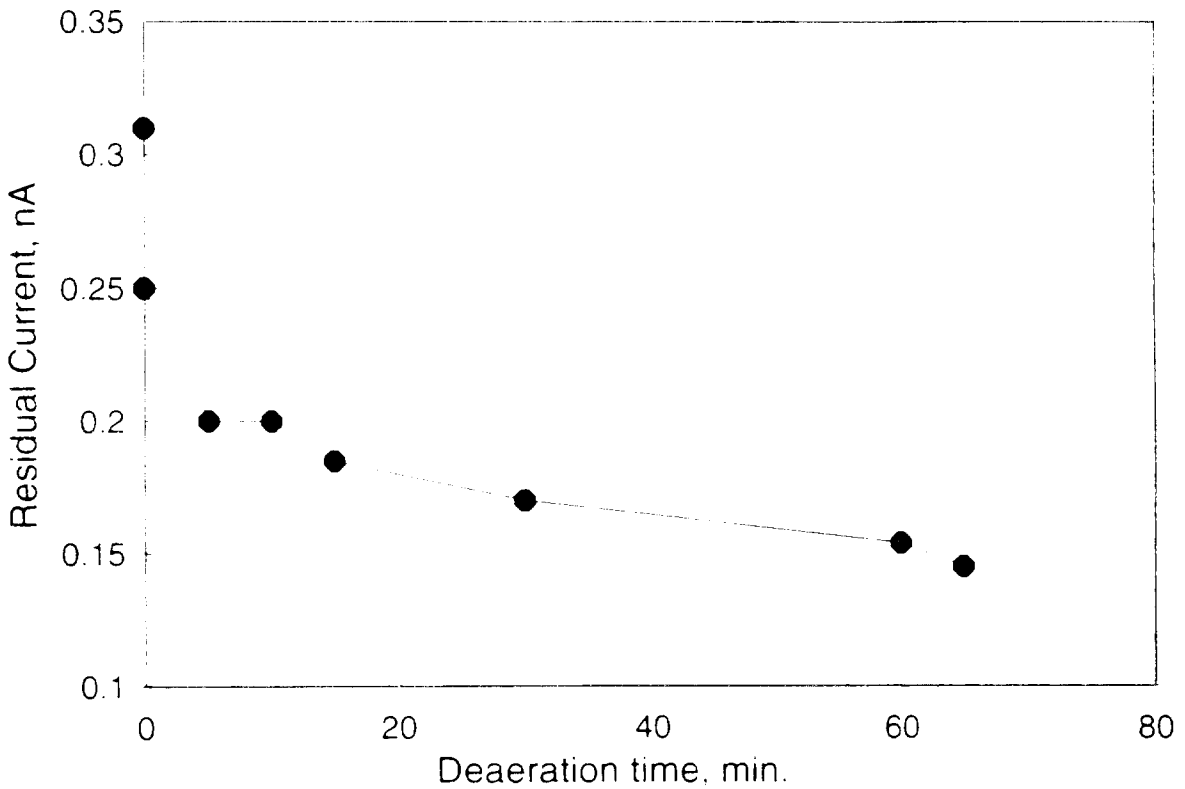

Figure 2.6 Effect of oxygen on residual current at 0 V vs. Ag|AgCl in background voltammograms acquired at site 1.

A possibly more significant CV feature relating to the status of the Ir site is the increase in anodic current as the potential scan progresses from 0.0 V to +0.2 V. This increase in anodic current was evident in CVs acquired after the third day of soaking but its significance was not appreciated until impedance data began to show a potential dependence of the impedance. A potential dependence of impedance would be consistent with Ir oxide, not bare Ir metal. In order to evaluate the site for the presence of oxide, the potential window for voltammetry was extended to +0.6 V vs. Ag/AgCl to include the potential region where oxide related reactions might occur. Figure 2.7 shows two series of CVs of all the sites on the ribbon cable probe. One series was taken on day 3 over the narrow potential range used for Ru hexammine studies, and illustrates the increase in anodic current above 0.0 V. The other series, taken on day 35 over with the extended potential window, demonstrates that sites 1, 2, 5 and 6 are somewhat activated, with site 1 having the highest oxide charge. The oxide-like CVs are puzzling because the sites were never intentionally activated, and were not subjected to any potential excursions that are deemed necessary for activation. Moreover, only site 1 was tested extensively. The other sites had a single voltammogram taken between -0.4 and +0.2 V which ought not cause activation. Previous studies in this laboratory of other silicon-based probes with sputtered Ir sites have also shown spurious "activation" of sites, but there was more uncertainty about the status of the previous sites due to problems with encapsulation and electrolyte penetration. With this ribbon cable probe, we are more confident that the phenomenon is related to the Ir and/or something in our test procedure. We do not know if the oxide was present before testing began. Our standard CV protocol does not include scans beyond +0.2 V, which is not anodic enough to identify unambiguously the presence of an oxide layer. Neither should it produce an oxide layer. To resolve the issue of oxide origin, the sequence of voltammetric measurements in future studies will be modified to look specifically for oxide before any other tests are performed.

The CVs of the other two sites on the probe were atypical possibly because of bad contacts. The CVs of site 3 had the characteristic box shape of a pure capacitor with symmetry along the current axis. The CVs of site 4 were asymmetrical and skewed about the current axis but with current 10 times lower than the current at sites 1, 2, 5 and 6.

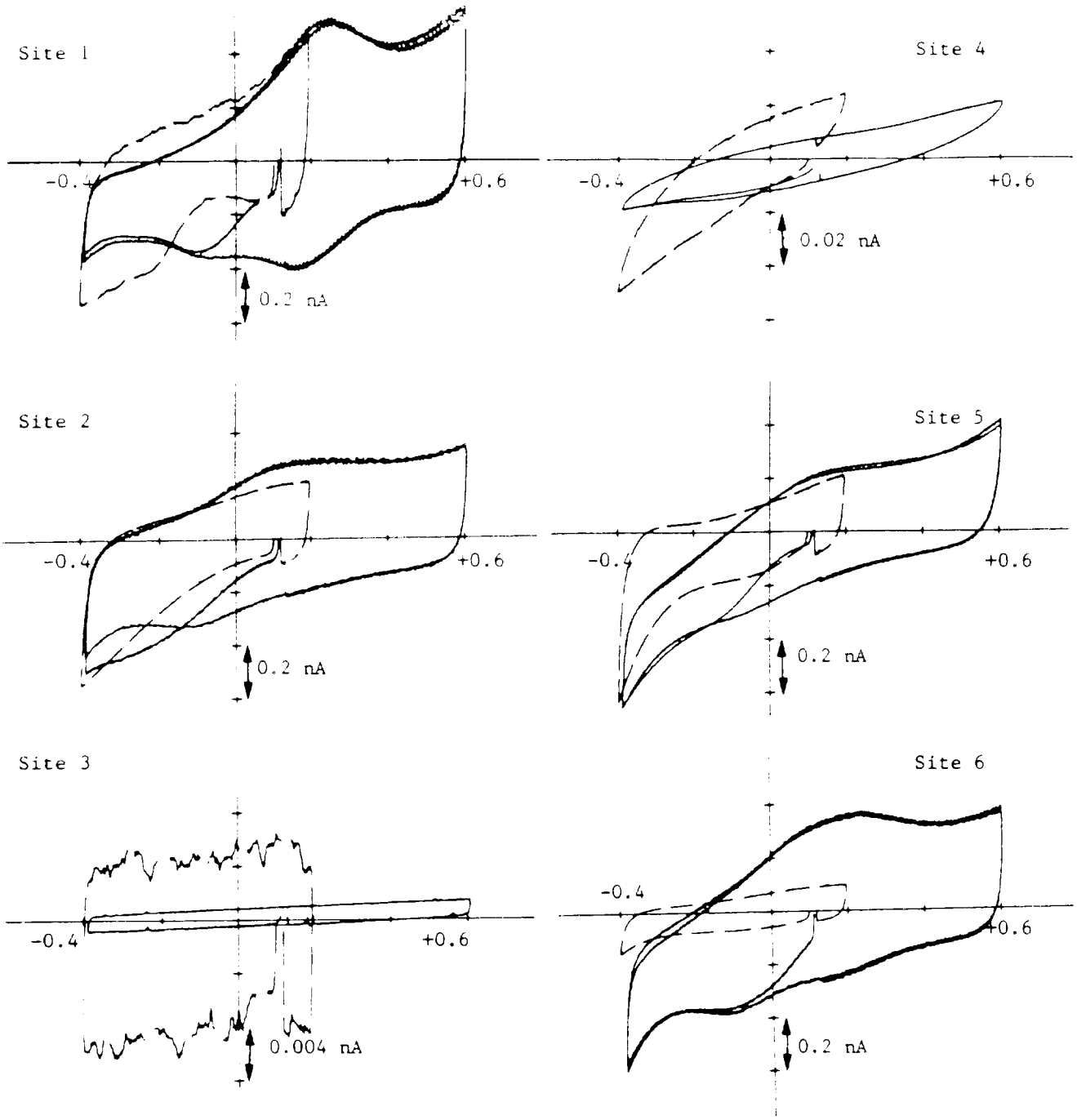

Figure 2.7 Voltammograms of all sites on U. Michigan ribbon cable demonstrating that some sites have become "activated". Day 3: broken line. Day 34: solid line. Electrolyte: deaerated PBS. Scan rate: 0.05 V/s. Potentials vs. Ag/AgCl.

Impedance Spectroscopy

Impedance spectra were acquired at site 1 on the ribbon cable at various times during the soak period and under different bias conditions. For this report only the impedance values at 1 kHz will be presented. Full frequency dispersions will be analyzed and presented in a future report. Table 2.4 lists the impedance values at 1 kHz as a function of applied bias potential and soaking time. The table also documents the chronology of tests performed on this site which may be important in diagnosing the changes in impedance which were observed. The first impedance spectrum was taken shortly after the ribbon was mounted in the test cell containing the Ru hexaammine solution. The impedance of ~ 1MΩ at 1 kHz was the highest value observed for the site, and probably was due to the short period of exposure to electrolyte solution with incomplete wetting of the surface. A second impedance spectrum taken on the following day under the same experimental conditions gave a value of 688 KΩ which is typical for an Ir site with these dimensions. Following this impedance measurement the probe was soaked overnight in dH_2O to remove all salt, and dried until the tests could be resumed. When the probe was again placed into solution, and impedance was taken with the site biased at −0.5 V vs. Ag/AgCl. This measurement gave a 1 kHz value of ~400 KΩ. On the following day, a series of impedance spectra were taken at a range of potentials from -0.2 V to +0.5 V, in random sequence. These impedance values show a marked variation from low to high values in inverse relationship to applied potential. This variation of impedance with potential is typical of activated Ir. At high anodic potentials, the oxide is electronically conductive. At low potentials, typically below 0 V vs. Ag/AgCl, the oxide has higher impedance due to lower conductivity of the lower valence form of the oxide. With longer soaking times, the difference in impedance between between high and low potentials becomes more pronounced. These differences may be related to the length of time the site was equilibrated at the bias potential before the impedance data were acquired. As indicated in the previous section, future studies will attempt to determine how and when the sites become "activated".

Table 2 4 Impedance at 1 kHz of site 1 on U Michigan ribbon cable-probe at different potentials and different times during soaking period

Soak Time (Days)	History	Potential, V vs Ag AgCl							
		-0 2	-0 1	0	0 1	0 2	0 3	0 4	0 5
0 2	Imped only				1028				
1	Study 1-Ru Impedance Dried 4 days				688				
0-0 5	Study 1-PBS Soak PBS								
1	Impedance								405 396
2	Impedance	457			393 232	204	219		198
3	Impedance CVs all sites		432	377				242	
	Study 2-Ru								
8	Study 2-PBS Impedance							189	190
9	Impedance					217 213	233		
15	Impedance	502					230	234	210
20	Impedance	610	631	552	367				
25	Impedance	625							

Dual Hat-Pin Microelectrode

The dual hat-pin Ir microelectrode from the Laboratory for Neural Control at NINDS was examined by SEM at the end of the long term soak test described in Quarterly Progress Reports No 2 and No 4 One of the electrode tips could not be seen clearly because it curved away from the line of sight However, it was possible to examine the other tip in a couple of different orientations This examination demonstrated several defects which are illustrated in Figure 2 8A and B Figure 2 8A shows that the wire was severely bent and the Parylene appears separated from it Figure 2 8B was taken at a slightly different angle and illustrates clearly that there is a groove in the wire which runs lengthwise almost to the tip This longitudinal groove is a

manufacturing defect which has been reported previously both by EIC and by the Laboratory for Neural Control. Because pre-testing photomicrographs of the electrode showed that the tips were straight, we hypothesize that the bending of the tip was accidentally produced at some time during the long term soak test, possibly as a result of a pipette or reference electrode brushing against the tip when the electrochemical cell was prepared for measurements. The electrochemical data indicated good stability of both tips up to the day 86 test protocol., following which there was an abrupt change in electrochemical surface area. Possibly that change in ESA reflected the damage to the electrode seen in the SEMs at the end of the soak period.

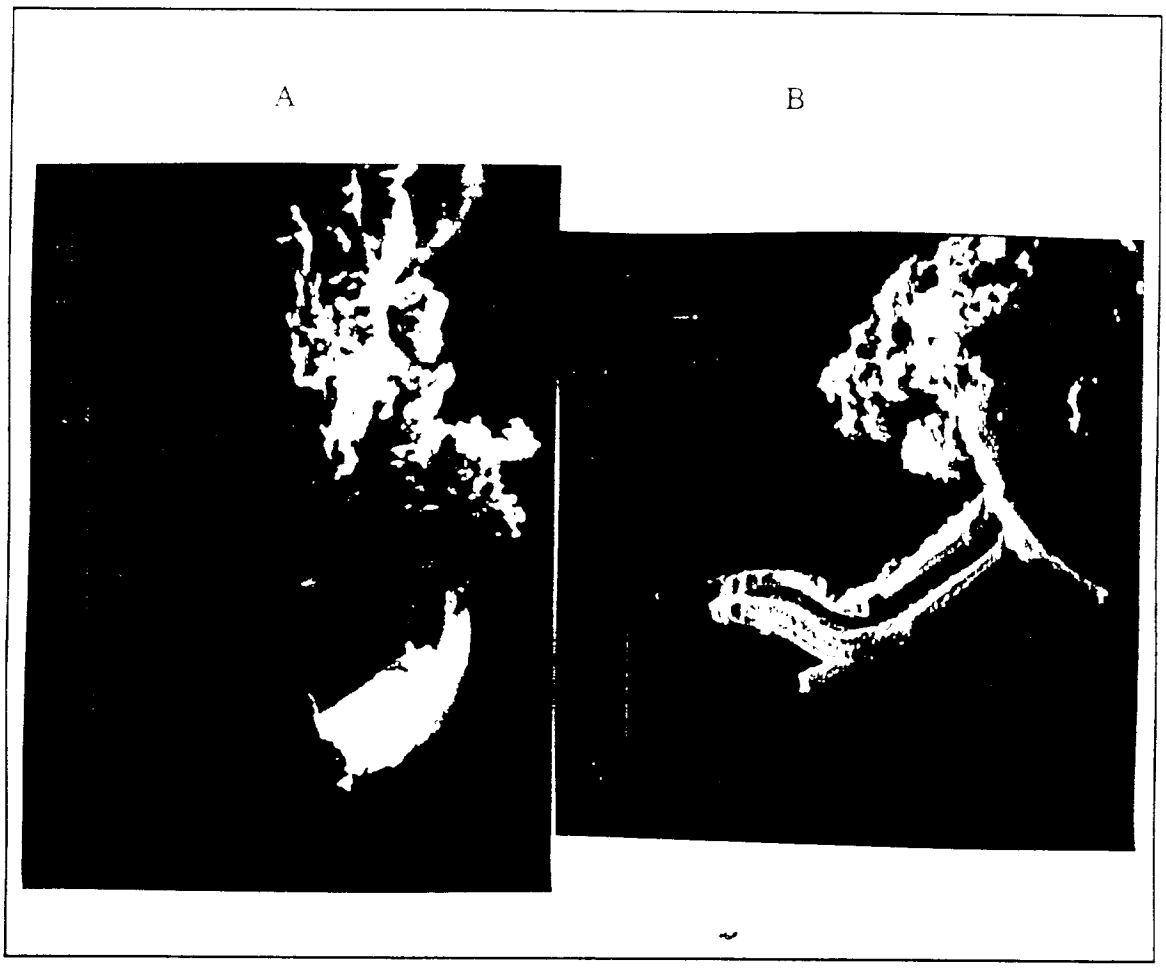

Figure 2.8 Scanning electron micrographs of one of the "hat-pin" microelectrodes on the dual hat-pin array, Bak #11. Note the longitudinal groove which extends almost to the tip of the electrode. The groove is a manufacturing defect.

3.0 CHARGE INJECTION STUDIES

During this quarter video microscopy was utilized to monitor the activation of sputtered Ir sites via their color change during potential cycling. The effect of charge injection on sputtered Ir and activated sputtered Ir was also examined using video microscopy in combination with monitoring of potential excursions during stimulation, and cyclic voltammetric assessment of oxide charge capacity. Video microscopy enables visualization of the onset of gas evolution, the loci of gas bubble formation at a microelectrode, and any changes in Ir or Ir oxide as a result of electrical stimulation. The first electrode evaluated was a U. Mich. multishank electrode, MS-56, with site geometric areas of 1728 μm^2. A site was activated by potential pulsing while being observed by video microscopy. Figure 3.1 illustrates the color changes observed at an activated site at two potentials. At sufficiently anodic potentials, e.g. >0.1V vs. Ag/AgCl, the site appears dark, and below that potential it appears light. This color change is due to the electrochromic property of Ir oxide. The potential-dependent color change permits us to evaluate the effect of stimulation parameters on the oxidation state of the oxide film.

Sites 4 and 5 on multishank electrode No. MS-54 were used in activation and stimulation experiments. The details of the stimulation experiments are summarized in Table 3.1 and the video observations are illustrated in Figures 3.2-3.7. Site 5 was activated prior to electrical stimulation. Site 4 was stimulated without being activated. Figure 3.2 illustrates the initial appearance of each of these sites. During stimulation of each site, the current was slowly incremented until bubble formation was observed by video microscopy and then it was held at that level for a short period of time.

The first observation of bubble formation at site 5 was with a cathodic pulse current of 276 μA. There were only three or four bubbles formed which were very small and localized to one edge of the site. These bubbles disappeared within a few seconds, and no additional bubbles were observed during the next 3 min. of stimulation at this current level. At an elapsed time of 7 min., the current was increased until at 376 μA bubbles were formed again at the same location. As was observed with the lower current, the bubbles disappeared within a few seconds. The current was increased for a third time, to 500 μA, at which time bubbles were observed briefly at

the same location on the site. The site was stimulated for an additional 11 minutes at the 500 μA level with no further bubble formation. However, the site became visibly darker, particularly around its perimeter. The darker color at the site edges is due to formation of additional Ir oxide during the stimulation experiment. The peak cathodic potential attained during stimulation with 500 μA pulses was ~-1.76 V vs. Ag/AgCl which is considered to be considerably beyond the "safe" limit based on the cyclic voltammetry potential window for H_2 production. The interpulse potential of +0.46 V vs. Ag/AgCl could account for the dark coloration at the edges of the site, with the potential cycling during stimulation pulses accounting for the growth of additional oxide.

Table 3.1 Charge injection studies of Ir sites on U. Mich. MS-54. A(geom)=1728 μm^2.

Site No.	Pulse Protocol	I	Q		R_A	IPP	ΔE	Result
	elapsed time min:sec	(μA)	(nC)	μC/cm²	(kΩ)	(V)	(V)	color/gas
Site 5 Activated	CF, cap. cpled., 50 pps 0:0	20	4	231	N.M.	N.M.	N.M.	dark, no effect
	2:49	130	26	1500	N.M.	N.M.	N.M.	dark,no effect
	4:00	276	55	3200	4	0.18	-2.11	dk; bubbles briefly
	7:00	376	75	4350	4	0.32	-2.22	dk; few bubbles briefly
	11:00	500	100	5787	4.8	0.46	-2.22	dk;few bubbles briefly
	22:08	"	"	"	N.M.	N.M.	N.M.	darker
Site 4 Unactivated	CF, cap.cpled., 50 pps 0:0	10	2	116	13.6	0.32	-1.2	light color
	2:09	100	20	1160	9.7	0.57	-1.52	light; many bubbles
	2:15	"	"	"	"	"	"	bubbles gone
	10:03	240	48	2778	8.2	0.6	-2.55	light;few bubbles briefly
	10:58	"	"	"	"	"	"	dark
	12:05	"	"	"	"	"	"	darker

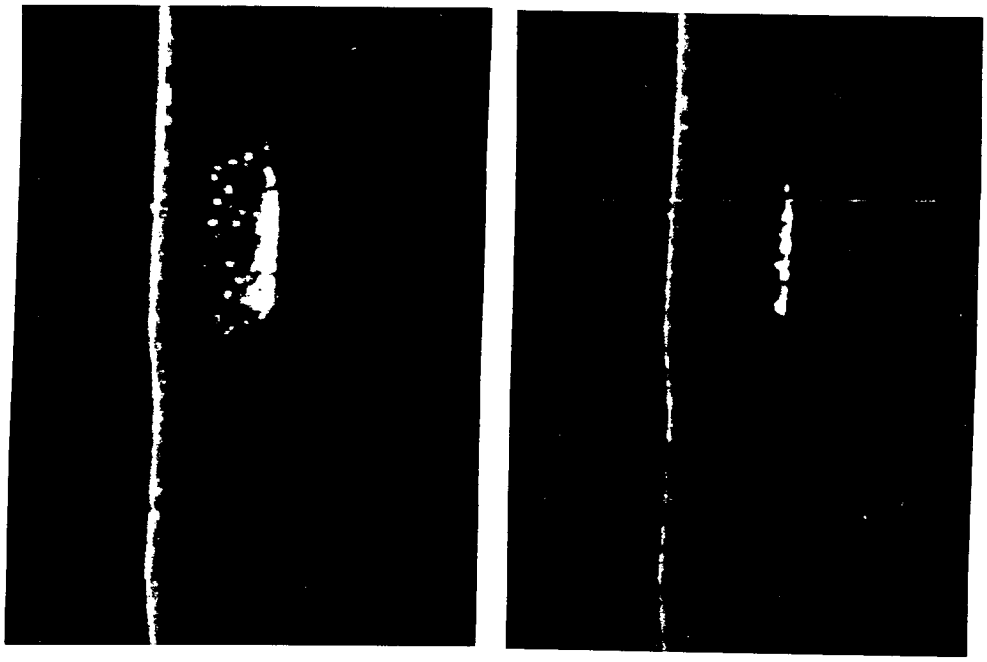

Figure 3.1 Activated site on MS-56 at two different potentials illustrating the electrochromic property of activated Ir. Left: -0.6 V vs. Ag/AgCl, reduced. Right: +0.6 V vs. Ag/AgCl, oxidized.

Figure 3.2 Sites 4 (left) and 5 (right) on MS-54 prior to stimulation experiment. Site 4 is not activated, site 5 is activated. Note the difference in color/contrast of the two sites.

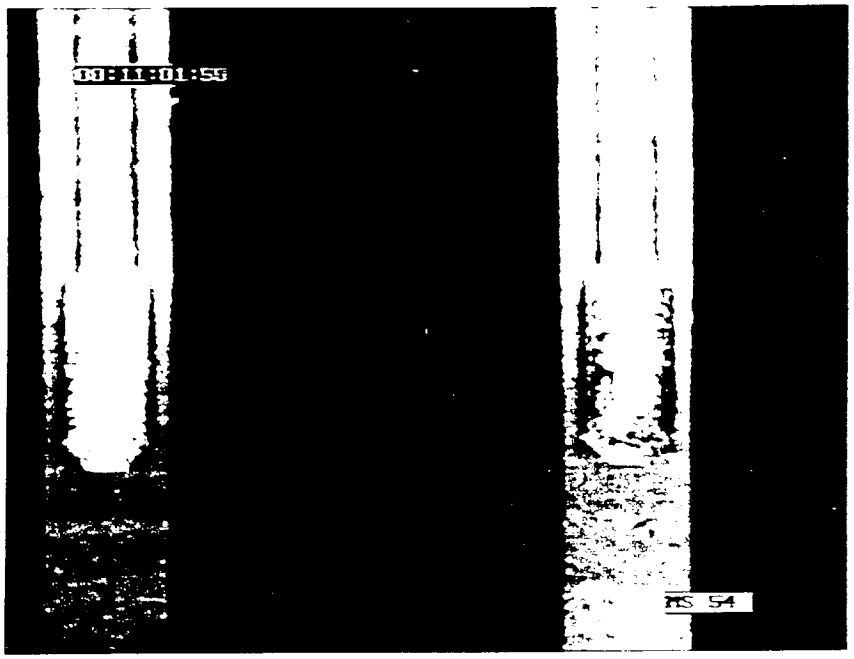

Figure 3.3 Site 5 (right) on MS-54 with 500 µA pulse current applied (see Table 3.1). Note small bubbles at left side of site. Bubbles were only seen at these loci, and they disappeared within a few seconds of continued stimulation.

Figure 3.4 Site 5 (right) on MS-54 after stimulating for 11 min with 500 µA pulse current applied (see Table 3.1). Note the very dark regions around the periphery of the site. This suggests that these edges are more activated that the center of the site, evidence for non-uniform current distribution.

A similar sequence of observations was made for site 4 which was stimulated without prior activation. Bubble formation at this site occurred at a lower stimulation current (100 μA), and the bubbles completely surrounded the perimeter of the site. These bubbles also disappeared within a few seconds and did not reappear until the current was increased again. After 8 min additional stimulation at 100 μA, the current was increased to 240 μA, at which time bubbles were again observed at the edge of the site but were fewer in number than were observed in the first bubbling episode. Stimulation at this current level was contined for an additional 3 min. during which time the site became visibly darker, consistent with the presence of an oxide film in a high valence state. The potential excursions during the pulse went to ~-2 V vs. Ag/AgCl, with an interpulse potential of +0.6 V vs. Ag/AgCl. The anodic interpulse potential could account for the dark color of the site, but the formation of oxide most likely occured via the potential cycling between -2 V and +0.6 V as a result of stimulation.

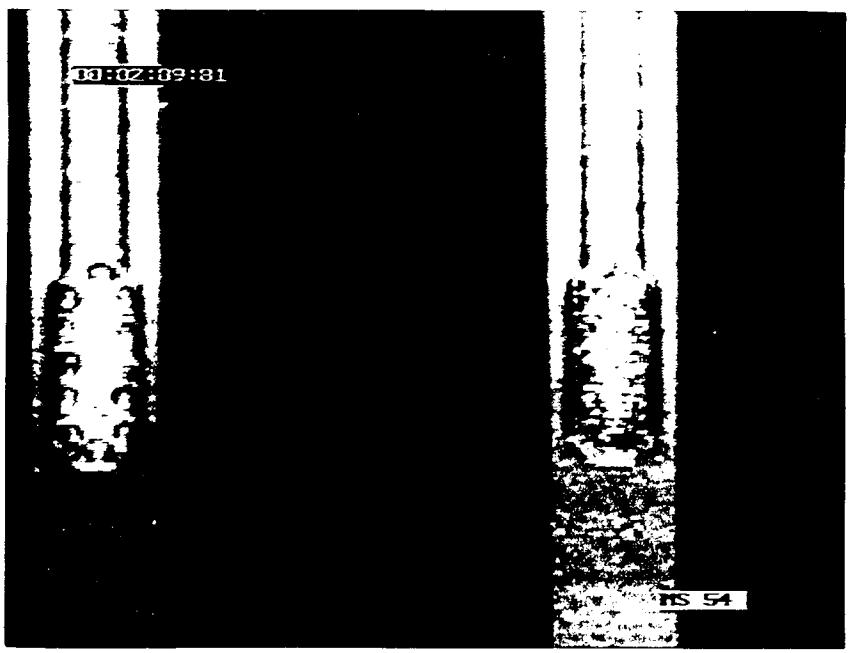

Figure 3.5 Site 4 (left) on MS-54 with 100 μA pulse current applied (see Table 3.1). Note that the bubbles are located exclusively at the edge of the site, and that there are more bubbles than were produced on site 5 with a higher current. Bubbles disappear within a few seconds.

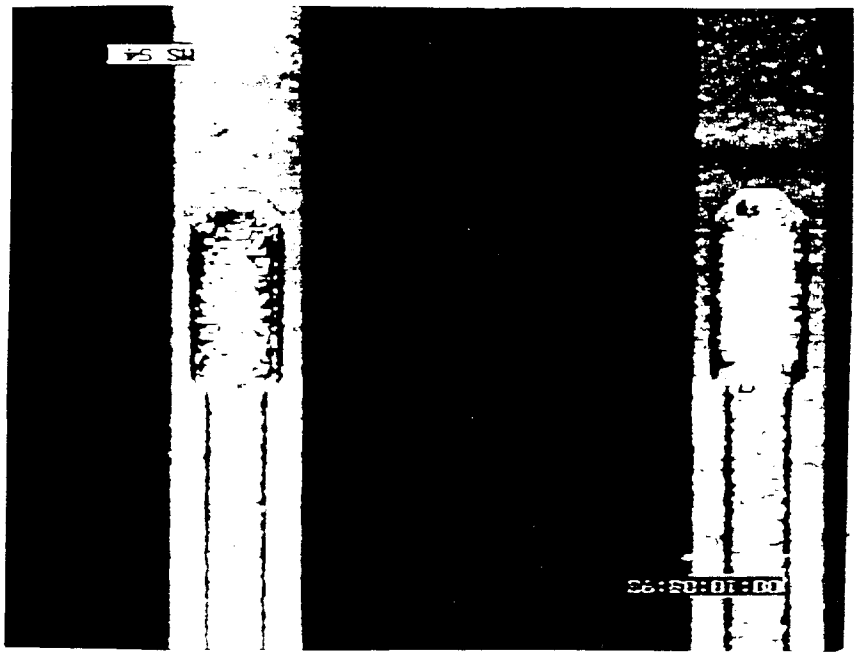

Figure 3.6 Site 4 (left) on MS-54 with 240 μA pulse current applied (see Table 3.1). Note that there are fewer bubbles than in Figure 3.5, but they are also located at edge of site

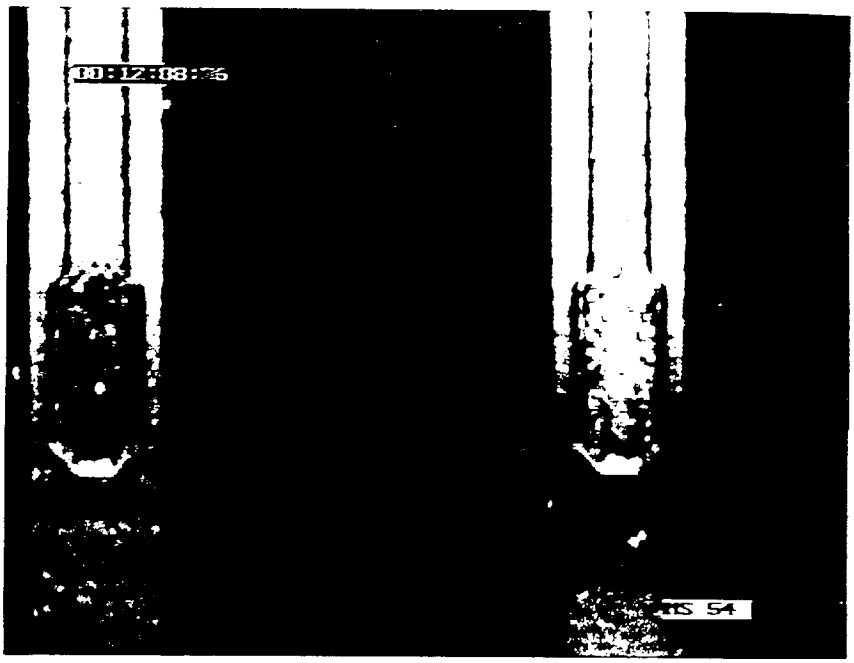

Figure 3.7 Site 4 (left) after 2 min. stimulation with 240 μA pulse current applied. Note how dark the site is due to oxide formation, i.e., Ir activation, as a result of high charge density stimulation

Cyclic voltammetry of the sites after stimulation indicated growth of oxide on both sites (Fig.3.8). Scanning E.M. indicated no disruption of the film of site 5 (Fig. 3.9), however the film on site 4 appeared cracked and disrupted, consistent with presence of a thick oxide (Fig.3.10).

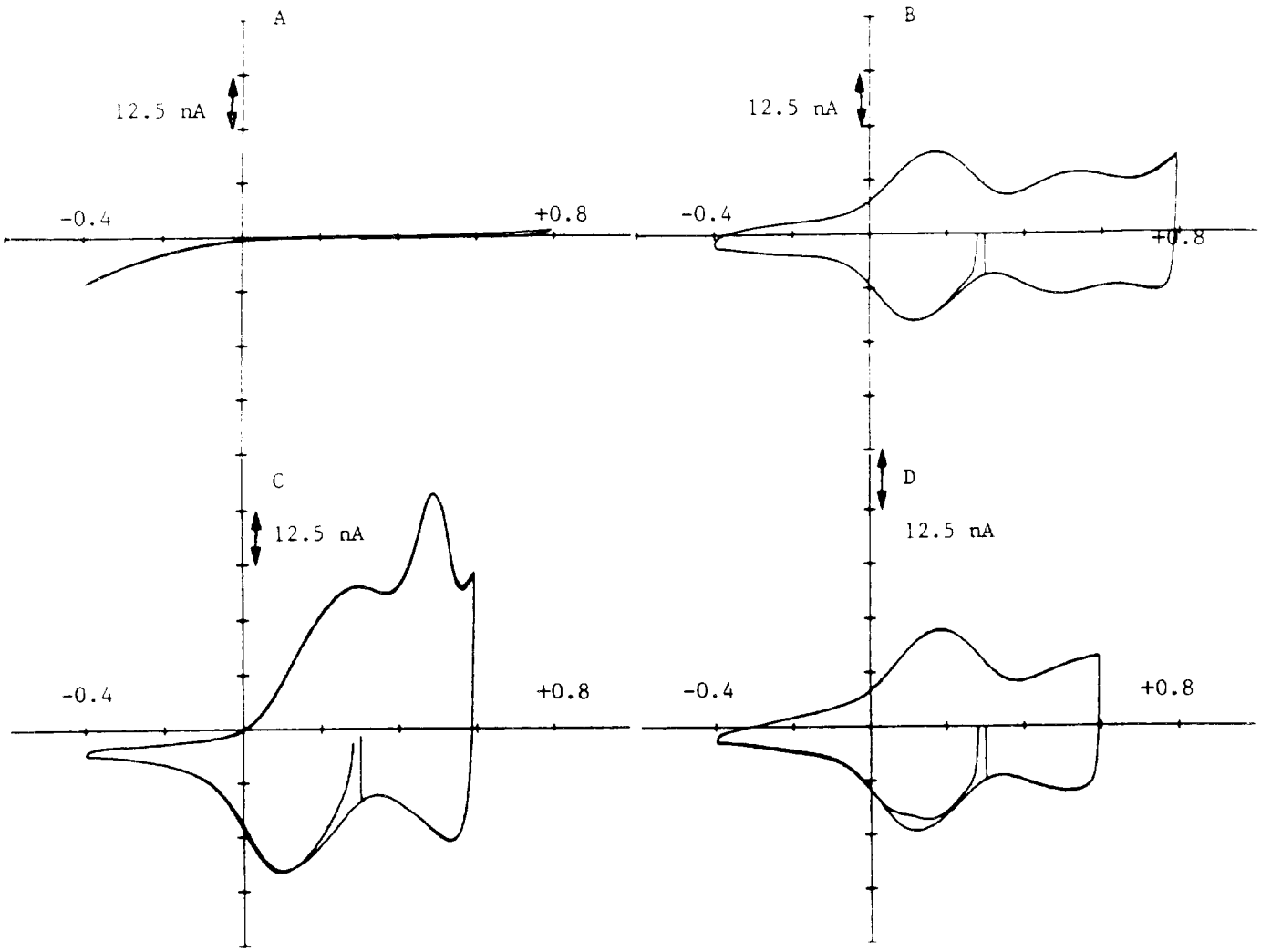

Figure 3.8 Cyclic voltammograms of sites on MS-54 demonstrating changes in voltammetric behavior due to activation, stimulation, and activation plus stimulation. Electrolyte: aerated PBS. Scan rate: 0.05 V/s. Potentials vs. Ag/AgCl.
A Site 3, before activation (given as example of unactivated site).
B Site 3, after activation (given as example of activated site).
C Site 4, unactivated, after pulse stimulation.
D Site 5, activated, after pulse stimulation.

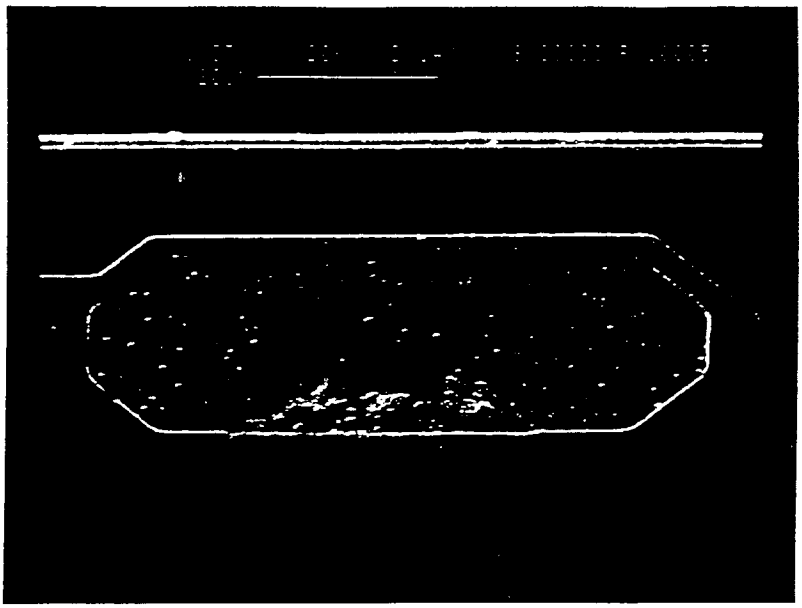

Figure 3.9 SEM of site 5 on MS-54 after stimulation experiments. Note that the site is flat, adherent to the substrate, and without any major defects. There is some deposit at the lower edge of the site as it is oriented in the photograph. This area corresponds to the location of some of the bubbles seen in Figures 3.3, but the identity of the deposit is not known.

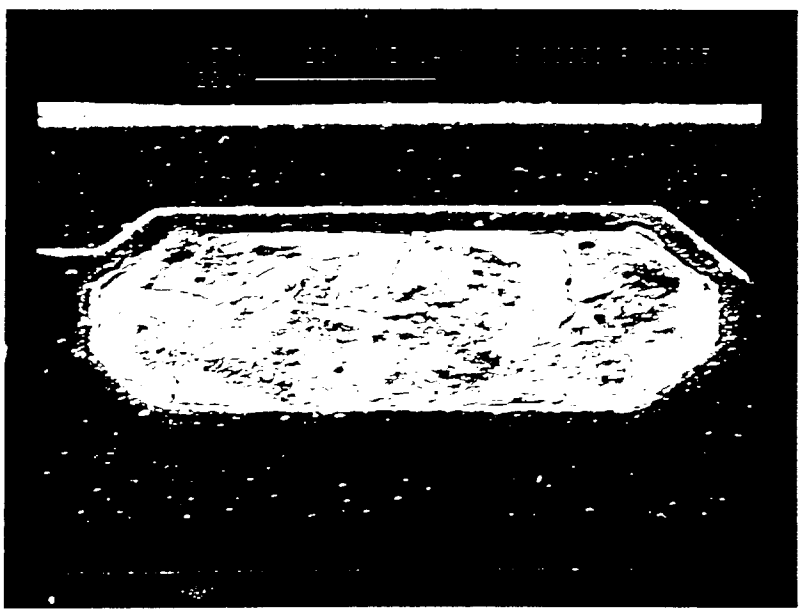

Figure 3.10 SEM of site 4 on MS-54 after stimulation experiments. Note the cracked and disrupted film structure which is consistent with thick Ir oxide. The formation of a thick oxide was also observed by cyclic voltammetry.

4.0 WORK FOR NEXT QUARTER

Two additional cell assemblies will be fabricated to enable simultaneous long term stability tests on multiple ribbon cable probes. We will attempt to identify the source of the spontaneous "activation" that was observed in CVs acquired late in the soak test period, and modify our test protocol to identify when this activation was acquired. Charge injection studies will be continued with the goal being to determine effect of electrode geometry on current distribution. Waffle electrodes from U. Michigan have been submitted for evaluation of charge injection properties and stability of oxide charge capacity. Charge injection tests on these electrodes have been initiated and results will be presented in the next quarterly progress report.

5.0 REFERENCES

1 Twardoch, U. M. 1994. Integrity of ultramicrostimulation electrodes determined from electrochemical measurements. J. Applied Electrochem. **24**:835-857.